Research Square

Preprints are preliminary reports that have not undergone peer review.
They should not be considered conclusive, used to inform clinical practice,
or referenced by the media as validated information.

Attosecond timing jitter in millimeter waves via Kerr optical frequency division

Antoine Rolland

arolland@imra.com

IMRA America, Inc. https://orcid.org/0000-0002-3214-0062

Scott Egbert

IMRA America, Inc.

Brendan Heffernan

IMRA America, Inc. https://orcid.org/0000-0002-0319-1602

James Greenberg

IMRA America, Inc. https://orcid.org/0000-0001-7731-257X

William McGrew

IMRA America, Inc.

Article

Keywords: optical frequency combs, phase noise metrology, microcombs, non linear optics

Posted Date: March 17th, 2026

DOI: https://doi.org/10.21203/rs.3.rs-8902301/v1

License: This work is licensed under a Creative Commons Attribution 4.0 International License.
Read Full License

Additional Declarations: There is **NO** Competing Interest.

Version of Record: A version of this preprint was published at Nature Photonics on September 23rd, 2026. See the published version at https://doi.org/10.1038/s41566-026-02014-x.

Attosecond timing jitter in millimeter waves via Kerr optical frequency division

Scott C. Egbert[1†], Brendan M. Heffernan[1†], James Greenberg[1], William F. McGrew[1], Antoine Rolland[1*]

[1]Boulder Research Labs, IMRA America, Inc., 1551 S Sunset St, Suite C, Longmont, Colorado, 80501, USA .

*Corresponding author(s). E-mail(s): arolland@imra.com;
[†]These authors contributed equally to this work.

Abstract

Millimeter-wave oscillators are essential for communication, radar, spectroscopy, and emerging photonic–electronic systems, yet their spectral purity remains constrained by noise processes intrinsic to direct generation at the carrier frequency. Here we demonstrate a fundamentally different approach that circumvents these limits by optically dividing a multi-terahertz reference to the millimeter-wave domain using Kerr soliton dynamics. A 3.3 THz dual-wavelength Brillouin laser injection-locks a chip-scale Kerr microcomb, enforcing exact optical frequency division to a 300 GHz repetition rate without electronic multiplication or feedback control. The resulting oscillator enters a previously inaccessible noise regime, exhibiting single-sideband phase noise of -152 dBc Hz^{-1} at a 1 MHz offset, corresponding to an unprecedented timing noise of 18 zs $Hz^{-1/2}$ for a directly measured photodetected microwave or millimeter-wave signal. Integration of the measured spectrum yields an rms timing jitter of 135 attoseconds from 1 kHz to 1 MHz. To directly resolve this performance, we implement cross-correlation phase-noise metrology at 300 GHz using independent photonic local oscillators. These results establish Kerr optical frequency division as a general and scalable route to millimeter-wave and sub-terahertz carriers whose coherence is no longer constrained by direct-generation limits, opening a new operating regime for photonic oscillators.

Keywords: optical frequency combs, phase noise metrology, microcombs, non linear optics

Introduction

Oscillators are the engines of coherence in science and technology. They set the cadence for digital communication, define the resolution of radar and spectroscopy, and underpin the synchronization of clocks and sensors across vast scales [1, 2]. From radio to optical, progress in oscillator performance has repeatedly opened new frontiers, including global navigation, high-speed networks, and tests fundamental physics [3, 4]. Yet, as carrier frequencies climb into the millimeter-wave and terahertz ranges, where new applications in high-capacity wireless [5], coherent imaging [6], molecular spectroscopy [7, 8] and astronomy [9, 10] demand ever purer signals, fundamental noise constraints limit oscillator coherence.

This limitation is especially acute near 300 GHz, a band of growing technological importance that sits between electronic and photonic domains. At such frequencies, available sources can generate carriers but not sustain the spectral purity required for many cutting-edge applications. This challenge now extends beyond signal generation to signal acquisition: recent advances in photonic-electronic analogue-to-digital converters (ADCs) have pushed acquisition bandwidths to and beyond 300 GHz, making oscillator coherence and timing jitter a primary performance bottleneck rather than the front-end electronics themselves [11]. In practice, phase noise at Fourier frequencies from approximately 1 kHz to 1 MHz dominates the integrated timing jitter, directly limiting sampling fidelity, coherence time, and achievable resolution. Random fluctuations in phase redistribute energy into noise sidebands, shortening coherence times and degrading timing stability. These effects are rooted not only in technical imperfections but also in fundamental noise processes, notably the Schawlow–Townes linewidth [12], which has long limited the performance of electronic multipliers and photonic synthesizers. Dual-wavelength Brillouin lasers (DWBLs) exemplify this constraint, exhibiting a fundamental phase-noise floor at intermediate Fourier frequencies [13, 14].

DWBL systems exploit stimulated Brillouin scattering in fiber to generate two mutually coherent optical tones whose beat yields a millimeter-wave carrier. Although such sources can generate 300 GHz signals with low phase noise, technical noise dominates below $\approx$1 kHz offset, while spontaneous scattering from thermally populated acoustic phonons imposes a fundamental noise floor up to the measurement shot-noise limit [15]. Because this quantum noise is set by cavity parameters rather than by the optical spacing, it does not increase in absolute terms with larger separations. This suggests that increasing the dual-wavelength separation combined with division to the desired carrier frequency will reduce the fractional impact of the Schawlow-Townes limit and yield a lower-phase noise source.

Kerr-nonlinear dynamics in microresonator frequency combs have enabled optical frequency division and precision timing at repetition rates near 300 GHz, including recent demonstrations of attosecond-level relative timing synchronization between chip-integrated microcombs [16]. While these advances highlight the potential of Kerr-mediated division for large-scale timing distribution, they primarily address relative timing correlations rather than the absolute spectral purity and timing noise of a synthesized millimeter-wave carrier. Here, we address this gap by implementing Kerr-induced optical frequency division (Kerr OFD) of a state-of-the-art 3.3 THz dual-wavelength Brillouin laser using a microresonator frequency comb, driving division into a qualitatively new noise regime at 300 GHz where performance is governed by fundamental detection limits rather than reference or servo noise [17–20].

In this work, we implement Kerr OFD using the two optical lines of a 3.3 THz DWBL to simultaneously pump and injection-lock a microresonator comb with a 300 GHz repetition

rate. The resulting soliton pulse train is dispersion-compensated and photodetected in a uni-traveling-carrier photodiode (UTC-PD), yielding a spectrally pure 300 GHz carrier. Dividing from 3.3 THz down to 300 GHz reduces the influence of fundamental noise processes in direct proportion to the frequency ratio. The oscillator achieves phase noise of −135 dBc/Hz at 10 kHz and −152 dBc/Hz at 1 MHz offset. Integration of the measured spectrum from 1 kHz to 1 MHz yields an RMS timing jitter of 135 as. At 300 GHz, this corresponds to a timing-noise floor of approximately 18 zs/$\sqrt{\text{Hz}}$, below even the quietest signals achieved with full optical frequency division [21], and realized here without the complexity of a self-referenced frequency comb or servo-controllers. Direct verification was obtained using the first application of cross-correlation phase-noise measurements in the millimeter-wave regime with photonics-based local oscillators. Together, these results establish a new benchmark in oscillator spectral purity and show that attosecond-level integrated timing jitter can be realized in the sub-terahertz domain with a simplified architecture.

Oscillator architecture

The oscillator architecture is based on optical frequency division of a multi-terahertz optical reference to the millimeter-wave domain using Kerr soliton dynamics, as illustrated in Fig. 1A. Additional details, along with a detailed schematic of the complete Kerr OFD experimental system, are provided in the Methods Section as well as the Supplementary Information. A dual-wavelength Brillouin laser (DWBL) provides two mutually coherent optical tones, denoted ν_p and ν_i, separated by $\Delta\nu = 3.3$ THz, which together form an optically-carried terahertz reference. Dual-tone Brillouin lasers are known to exhibit exceptionally low phase noise at large optical separations and, as demonstrated here, operate without electronic phase-locked loops [13, 14].

The two optical tones are simultaneously coupled into a high-Q microresonator supporting dissipative Kerr solitons. One tone, ν_p, pumps the resonator to initiate soliton formation, while the second tone, ν_i, injection-locks a higher-order comb mode through Kerr-induced synchronization [19]. In the injection-locked state, the injected tone ν_i, coincides with the comb line at optical mode $\mu_0 + N \cdot f_{\text{rep}}$, while the pump corresponds to mode μ_0. Injection locking therefore enforces an exact integer relationship between the optical separation and the soliton repetition rate, $f_{\text{rep}} = \Delta\nu/N$, such that the repetition rate inherits the phase noise of the optical reference reduced by the square of the division factor.

After optical frequency division in the microresonator, the soliton pulse train is spectrally conditioned to suppress the residual DWBL light and dispersion compensated before subsequent detection using a UTC-PD [22]. This dispersion compensation maximizes millimeter-wave power recovery during photodetection without affecting the frequency-division process or phase-noise scaling, enabling efficient readout at 300 GHz by preserving short optical pulse duration. Photodetection converts the repetition rate directly into a 300 GHz millimeter-wave carrier, completing the division from the optical domain to the millimeter-wave domain without electronic multiplication or high-bandwidth feedback control.

Figure 1B shows the optical spectrum of the soliton comb after suppression of the pump and injection tones. The spectrum exhibits a smooth sech^2 envelope and high optical signal-to-noise ratio across the comb lines, consistent with stable dissipative Kerr soliton operation.

Together, this architecture establishes Kerr optical frequency division as a general route to generating millimeter-wave carriers with coherence no longer constrained by the limits of direct electronic or photonic generation.

Injection locking of the Kerr soliton microcomb to the optical reference is verified by simultaneously monitoring the optical beat note between the injected laser ν_i and the corresponding soliton comb line at optical comb mode $\mu_0 + N \cdot f_{\mathrm{rep}}$, as well as the soliton repetition rate f_{rep} at 300 GHz (see green and blue traces, respectively, in Fig. 1C). The repetition rate (blue) is read out using an electro-optic (EO) comb-based frequency down-conversion technique [23]. The effective detuning between the injected optical tone ν_i and the targeted comb mode is swept by applying a controlled frequency modulation to the DWBL tones pumping the soliton comb (both ν_p and ν_i), preserving the optical separation and coherence of $\Delta\nu$, as described in the Supplementary Information.

Far from resonance, both the optical beat note (green) and the repetition rate (blue) follow the imposed scan, indicating free-running operation. As the injected optical tone ν_i approaches the targeted soliton comb mode, frequency pulling is observed and the optical beat note decreases to a minimum observable value of approximately 20 MHz. Below a critical detuning, the beat note (green) collapses to DC, indicating optical injection locking of the comb mode to the injected optical tone maintained over a range of about 280 MHz. The soliton repetition rate (blue) becomes insensitive to further tuning and clamps to the divided optical reference $\Delta\nu/N$, confirming Kerr OFD.

The large locking range compared to the intrinsic free-running drift enables stable injection-locked operation over hours without intervention under typical laboratory conditions. The injection-locking dynamics of the Kerr soliton repetition rate and the resulting exact optical frequency division law are quantitatively described by an Adler-type oscillator model, which defines a finite reference-tracking bandwidth and is presented in the Supplementary Information. There, we further include a comparison between this passive Kerr OFD injection-locking scheme and active phase-locked-loop (PLL)-based architectures, highlighting a 20–40 dB improvement in phase noise enabled by the large (~280 MHz) injection-locking bandwidth.

Phase Noise of Optical Division

Having established robust synchronization of the soliton microcomb to the Brillouin reference, we next examine the noise processes that ultimately limit the spectral purity of the divided signal. Throughout this section, phase noise is quantified by the single-sideband phase-noise power spectral density $S_\phi(f)$, expressed in units of dBc/Hz as a function of Fourier frequency f [24]. Figure 2A summarizes the impact of DWBL optical frequency separation $\Delta\nu$ on $S_\phi(f)$, comparing $\Delta\nu_{300\,\mathrm{GHz}}$ (red) and $\Delta\nu_{3.3\,\mathrm{THz}}$ (black), together with the Kerr optical frequency–divided output at $f_{\mathrm{rep}} = 300$ GHz (blue).

At Fourier frequencies below approximately 1 kHz, the phase-noise spectrum is dominated by environmental perturbations such as thermal drift and acoustic fluctuations. These contributions follow power-law dependencies of the form $S_\phi(f) \approx b_{-3,-4} f^{-3,-4}$ and scale quadratically with the optical separation $\Delta\nu$. As a result, increasing $\Delta\nu$ inevitably raises the low-offset phase-noise floor, such that $\Delta\nu_{3.3\,\mathrm{THz}}$ exhibits higher low-frequency noise than

$\Delta\nu_{300\,\mathrm{GHz}}$. This behavior reflects the enhanced sensitivity of widely separated optical tones to environmental perturbations rather than a fundamental limitation of optical frequency division.

At higher Fourier frequencies, however, the phase noise is governed by the quantum-limited linewidth of the optical cavity and follows $S_\phi(f) \approx b_{-2} f^{-2}$. In contrast to the low-frequency technical noise, the coefficient b_{-2} depends on the cavity linewidth and optical output power but is largely independent of the optical separation. Consequently, increasing $\Delta\nu$ does not reduce sensitivity to low-frequency technical drift after division. However, when a large optical separation such as $\Delta\nu_{3.3\,\mathrm{THz}}$ is divided down to $f_{\mathrm{rep}} = 300$ GHz, both the environmental noise and the fundamental Schawlow–Townes noise floor are suppressed by the square of the division factor, as indicated by the blue trace in Fig. 2A. At the highest Fourier frequencies (tens of megahertz), the measured phase noise is ultimately limited by the photodetection floor.

When the soliton repetition rate is constrained by $f_{\mathrm{rep}} = \Delta\nu_{3.3\,\mathrm{THz}}/N$, optical frequency division reduces the phase noise of the repetition rate by a factor N^2, corresponding to a reduction of $20\log_{10} N$ in phase noise (dBc/Hz) relative to direct generation of a 300 GHz tone using $\Delta\nu_{300\,\mathrm{GHz}}$. This scaling enables Kerr OFD to surpass the spectral purity achievable with a conventional dual-wavelength Brillouin laser operating directly at millimeter-wave spacings.

Because the resulting 300 GHz phase noise lies below that of any available reference oscillator at the same frequency (Fig. 2A), direct measurement is non-trivial. To verify the spectral purity in this regime, we implement cross-correlation phase-noise metrology [25] at millimeter-wave frequencies, benchmarking the Kerr OFD oscillator against two independent 300 GHz local oscillators derived from separate DWBL, as shown in Fig. 2B. Both beat signals are detected, mixed to baseband, digitized, and processed by digital cross-correlation. Because the noise of the two DWBL references is statistically uncorrelated, cross-spectral averaging suppresses their contribution, yielding a reference-free measurement of the DWBL-injected Kerr OFD oscillator phase noise. The same averaging also rejects uncorrelated noise from the measurement chain itself, including mixer conversion loss and flicker, amplifier flicker and noise figure, and digitizer background. This enables phase-noise characterization below the Schawlow–Townes limit of a single DWBL and beyond the resolution of conventional metrology hardware.

The measured single-sideband phase-noise spectra are presented in Fig. 2C. We first plot the free-running phase noise of the Kerr microcomb repetition rate (green), which exhibits a $1/f^3$ spectrum characteristic of uncompensated technical, acoustic, and thermodynamic fluctuations. Injection locking constitutes a form of passive synchronization, formally equivalent to a first-order phase-locked loop, such that the injected reference suppresses low-frequency noise while leaving a residual contribution determined by the free-running spectrum and the finite correction bandwidth, as described in the Supplementary Information.

When operated under Kerr OFD, the resulting 300 GHz oscillator (blue) exhibits a dramatic suppression of phase noise, reaching -135 dBc/Hz at a 10 kHz offset and -152 dBc/Hz at 1 MHz (the cross-correlation measurement bandwidth), all without a servo bump. This performance is in close agreement with the division-scaling analysis of Fig. 2A and represents a 75 dB reduction relative to the free-running microcomb at a 10 kHz offset. For Fourier frequencies above approximately 1 kHz, the Kerr OFD oscillator lies well below the noise floor of the best directly generated 300 GHz signals derived from DWBL local oscillators (red) and closely follows the quantum-limited performance expected from a $\Delta\nu_{3.3\,\mathrm{THz}}$ Brillouin spacing scaled to 300 GHz (dashed black, measured experimentally and reported in [14]).

In the present experiment, a UTC-PD operated at 4 mA photocurrent delivers approximately 50 µW of radiated power at 300 GHz, corresponding to a thermal noise floor near −164 dBc/Hz and a photodetection white-noise floor of approximately −152 dBc/Hz (see Supplementary Material). At lower Fourier offsets, the oscillator inherits residual acoustic and thermal fluctuations associated with the large optical reference spacing, consistent with the scaling behavior discussed in Fig. 2A. At a 10 kHz offset, Kerr OFD yields ≈20 dB reduction in phase noise relative to direct 300 GHz DWBL generation, demonstrating that the Schawlow–Townes limit associated with direct millimeter-wave generation has been substantially suppressed by division.

The timing jitter consequences of Kerr OFD are shown in Fig. 2D. Integration of the measured phase-noise spectra from 1 kHz to 1 MHz yields a total root-mean-square (RMS) timing jitter of 135 as for the Kerr OFD oscillator, compared to 395 as for a 300 GHz DWBL oscillator. The separation between the two curves persists across the entire integration bandwidth, indicating that the improvement is broadband rather than confined to a narrow frequency range.

A complete breakdown of the integrated phase variance by Fourier frequency band is summarized in Table 1. The dominant contribution arises from low-frequency DWBL noise between 10 Hz and 100 Hz, 90.8 fs of timing jitter or 99.5% of the total jitter from 10 Hz and 1 MHz. This noise can be significantly reduced by locking the oscillator to a stable reference, such as a molecular transition, as was shown in ref. [8], or a microwave standard [26, 27] using only a relatively slow (e.g. kHz) PLL bandwidth to suppress low-frequency noise while maintaining the advantageous phase noise at high Fourier frequencies derived from passive injection-locking.

Above 1 kHz, the residual timing fluctuations are strongly suppressed, with the 1–10 kHz, 10–100 kHz, and 100 kHz–1 MHz bands contributing only 132.7 as, 15.58 as, and 20.97 as, respectively. The total integrated jitter of 135 as from 1 kHz to 1 MHz firmly places the Kerr OFD-derived 300 GHz oscillator in the sub-femtosecond regime. Long-term stability of the Kerr OFD oscillator was independently verified using Allan deviation measurements, as described in the Supplementary Information.

Table 1 Integrated phase variance and RMS timing jitter by Fourier frequency band.

Offset band	Phase var. (rad^2)	Share of total	RMS jitter
10 Hz – 100 Hz	2.92×10^{-2}	0.995	90.8 fs
100 Hz – 1 kHz	1.47×10^{-4}	5E-3	6.44 fs
1 kHz – 10 kHz	6.25×10^{-8}	2E-6	132.7 as
10 kHz – 100 kHz	8.62×10^{-10}	3E-8	15.58 as
100 kHz – 1 MHz	1.54×10^{-9}	5E-8	20.97 as

Benchmarking phase noise and discussion

The Kerr OFD oscillator rivals, and at high Fourier offsets surpasses, the quietest signals produced by full lab-scale optical frequency division (OFD) [21], but with a fraction of the complexity. Whereas standard OFD techniques rely on ultrastable cavities, self-referenced

femtosecond combs, and multi-loop stabilization, the present system requires only two lasers, a fiber spool, a chip-scale resonator, dispersion compensation and a photodiode. This simplicity not only reduces size, weight, and power requirements, but also avoids excess noise introduced by active feedback, yielding a smooth spectrum and robust operation.

The same approach is, in principle, directly applicable to any repetition rate accessible to Kerr microcombs. Because such combs have been demonstrated from below 10 GHz to beyond 1 THz, the method presented here can extend across this entire range, providing a general route to low-noise carriers at microwave, millimeter-wave, and terahertz frequencies.

A 300 GHz carrier with attosecond-level integrated jitter can sustain dense data links, enable radars with micrometer precision, and support millimeter-wave spectroscopy at coherence levels previously unattainable. Fig. 3 places these results in context, comparing Kerr OFD of our DWBL to prior microcomb demonstrations for microwave and millimeter-wave generation [28–33]. When comparing timing noise, which scales inversely to the carrier frequency, the presented approach decisively surpasses all previous microcomb-based sources due to reaching this same photodetection limit using a 300 GHz carrier. The same plot also benchmarks against the quietest microwave signal ever realized with full OFD [21], showing that Kerr OFD combined with a DWBL source now reaches comparable or superior timing stability at high Fourier frequency (>10 kHz) with radically reduced complexity. Furthermore, we demonstrate, to our knowledge, the lowest photodetected timing noise ever measured at 18 zs/$\sqrt{\text{Hz}}$.

Equally important, this work expands the role of microcombs as much more than just a compact platform for integration. Here the high repetition rate and non-linear properties are leveraged to achieve performance that is transformative in their own right. The fact that such results are obtained with a chip-scale device merely underscores the promise of future integration, while this performance already establishes a new phase noise benchmark. As frequency combs reshaped optical metrology two decades ago, Kerr microcomb oscillators are poised to transform frequency synthesis across the microwave, millimeter-wave, and terahertz spectrum.

Methods

Experimental implementation of Kerr optical frequency division

The optical reference for Kerr optical frequency division (OFD) is provided by a self-injected dual-wavelength Brillouin laser (DWBL) operating near 1550 nm. The DWBL generates two mutually coherent Brillouin Stokes tones at optical frequencies ν_p and ν_i separated by $\Delta\nu = \nu_i - \nu_p = 3.3$ THz. A fraction of the Brillouin-shifted output is frequency-shifted back to the respective pump frequencies and re-injected into the pump lasers, passively stabilizing the mutual coherence and optical separation without the use of electronic phase-locked loops. Detailed descriptions of the DWBL operating principle and performance at terahertz spacings are reported in Refs. [13, 14].

The combined DWBL output is amplified to a total optical power of approximately 400 mW using a shared erbium-doped fiber amplifier (EDFA). A common amplifier is used to ensure that amplifier-induced phase fluctuations remain correlated between the two optical tones. Owing to the frequency-dependent EDFA gain profile, the injected-tone power is approximately 1% of the pump-tone power. To suppress amplified spontaneous emission (ASE) from the

EDFA, the two tones are spectrally cleaned using dense wavelength-division multiplexing (DWDM) filters configured as a dual bandpass filter that selectively transmits narrow spectral windows centered on ν_p and ν_i, as shown in the Supplementary Information. This filtering reduces broadband optical noise that can degrade soliton signal-to-noise ratio and enhance amplitude-to-phase conversion during photodetection.

Dissipative Kerr solitons are initiated using fast pump-frequency sweeping implemented via carrier-suppressed single-sideband modulation (CS-SSBM) [34]. Both optical tones ν_p and ν_i pass through the same CS-SSBM such that the applied frequency shift is strictly common-mode, leaving the optical separation $\Delta\nu$ unchanged. This common-mode actuation prevents differential phase noise originating from the voltage-controlled oscillator (VCO) drive from being imprinted onto the optical-difference reference.

The filtered and common-mode modulated tones are coupled into a high-Q microresonator waveguide supporting dissipative Kerr solitons. The lower-frequency tone ν_p pumps a cavity resonance to initiate soliton formation, while the higher-frequency tone ν_i is aligned to overlap a higher-order soliton comb mode. In the injection-locked state, the injected tone locks the targeted comb tooth via Kerr-induced synchronization [19], constraining the soliton repetition rate such that an integer number of comb modes spans the optical separation $\Delta\nu$. This enforces exact optical frequency division according to $f_{\mathrm{rep}} = \Delta\nu/N$. The finite reference-tracking bandwidth and its impact on phase-noise transfer are treated analytically in the Supplementary Information.

Following optical frequency division, residual pump and injection tones are rejected using DWDM filtering to prevent photodetector saturation. The resulting soliton comb is amplified using a second EDFA to an optical power of approximately 50 mW. Chromatic dispersion is compensated using a programmable optical filter (Finisar-waveshaper). The dispersion parameters are optimized by maximizing the recovered millimeter-wave power measured on a thermopile detector, exploiting the reduction in recovered microwave power under dispersive pulse broadening [35].

The dispersion-compensated soliton pulse train is incident on a uni-traveling-carrier photodiode (UTC-PD) (NTT IOD-PMJ-13001), which converts the repetition rate $f_{\mathrm{rep}} \approx 300$ GHz directly into a millimeter-wave carrier [22]. All measurements reported in the main text are performed at a fixed average photocurrent (≈ 4 mA) selected to minimize amplitude-to-phase (AM-to-PM) conversion while maintaining high carrier power.

Cross-correlation phase-noise measurement at 300 GHz

Phase-noise measurements of the Kerr OFD signal at 300 GHz are performed using a dual-channel cross-correlation technique operating in the baseband, as shown in Fig. 2B of the main text. Two independent local oscillators (LOs) at 300 GHz are generated from separate DWBL systems configured to produce the same optical frequency separation as the Kerr OFD output. Each DWBL LO is converted to a 300 GHz electrical signal by photodetection on a high-power UTC-PD biased at approximately 12 mA (NTT IOD-PMJ-24001) [36], yielding an output power of approximately 500 μW, sufficient to directly drive the LO ports of the frequency mixers (VDI WR3.4BAMULP).

The Kerr OFD signal under test is generated on an independent UTC-PD before being split and applied to the RF ports of the two nominally identical frequency mixers, producing two electrical beat notes in the baseband, with frequencies below approximately 200 MHz.

The two baseband signals are digitized and analyzed using a dual-channel frequency and phase analyzer (Microchip 53100A) capable of cross-spectral phase-noise measurements. The single-sideband phase-noise spectrum of the Kerr OFD signal is obtained by computing the cross power spectral density of the two baseband phase signals. Noise contributions that are uncorrelated between the two measurement channels, including additive noise from the mixers, baseband electronics, and the independent DWBL-derived LOs, are suppressed through cross correlation, while noise originating from the common Kerr OFD signal is retained. The free running microcomb phase noise was measured using a single-channel phase noise analyzer (Keysight SSA-X).

The same cross-correlation technique is also used to characterize the phase noise of the 300 GHz DWBL-derived local oscillators themselves. In direct single-channel measurements, the phase-noise floor is limited by the conversion loss and additive noise of the frequency mixers to approximately −145 dBc/Hz, preventing accurate extraction of the intrinsic DWBL noise. By driving the RF and LO ports of the two mixers with independent DWBL-derived signals and applying cross correlation, the uncorrelated mixer and baseband noise is suppressed, enabling measurement of the DWBL phase noise below the single-channel detection floor.

Because the DWBL-derived LOs are generated directly at 300 GHz and do not rely on electronic frequency multiplication, their phase noise is intrinsically low and largely uncorrelated between the two channels. As a result, the cross-correlation process converges rapidly. In practice, both the Kerr OFD and DWBL phase-noise spectra converge within approximately 5 minutes of averaging.

The validity of the cross-correlation measurement is verified by confirming the expected reduction of the uncorrelated noise floor with increasing averaging time, while the correlated phase noise of the signal under test remains unchanged. This procedure ensures accurate extraction of millimeter-wave phase noise over the full range of Fourier frequencies reported in the main text.

Operating conditions and measurement stability

All measurements reported in the main text are performed under steady-state injection-locked conditions, with the Kerr soliton operated near the center of the locking range. Under these conditions, the effective reference-tracking bandwidth is on the order of $f_c \approx 100$–300 MHz, as extracted from the locking plateau and described by the Adler-type model in the Supplementary Information.

The Kerr OFD signal under test is generated at a fixed average photocurrent of $I_{\mathrm{avg}} \approx 4$ mA on the UTC photodiode, corresponding to a recovered 300 GHz carrier power of approximately $P_\mu \approx 50$ μW. This operating point is experimentally identified as a local minimum in amplitude-to-phase (AM-to-PM) conversion, as discussed in the Supplementary Information, while still providing sufficient signal-to-noise ratio for low-noise detection.

For the cross-correlation phase-noise measurements, two independent local oscillators derived from the same dual-wavelength Brillouin laser (DWBL) optical reference are generated at 300 GHz using separate UTC photodiodes operated at $I_{\mathrm{LO}} \approx 12$ mA, yielding approximately $P_{\mathrm{LO}} \approx 500$ μW at each mixer local-oscillator port. These power levels are selected to ensure stable operation of the millimeter-wave mixers without saturation.

During phase-noise acquisition, all optical powers, bias currents, and locking conditions are held constant. We average each measurement nominally 5 minutes, sufficient to suppress

uncorrelated noise from the local oscillators while remaining short compared to any observable drift of the optical reference or injection-locking conditions. The derivation of the noise transfer functions and the role of cross correlation are detailed in the Supplementary Information.

Acknowledgments

We thank John Dorighi at Keysight Technologies for generously providing access to the SSA-X cross-correlator-based phase noise analyzer which enabled several key measurements in this work. We also acknowledge Hideyuki Ohtake and Yuki Ichikawa for their support throughout this work.

Author Contributions

A.R., B.H., and J.G. conceived and designed the experiments. S.E. developed the 3.3 THz reference. B.H. operated the Kerr optical frequency division. A.R. and J.G. constructed the 300 GHz cross-correlator, while B.H. and S.E. built and operated the dual-wavelength Brillouin lasers at 300 GHz that served as local oscillators. A.R., B.H., and S.E. carried out the measurements. All authors contributed to troubleshooting the technical challenges encountered during the experiments. W.M. provided theoretical insights. All authors participated in data analysis and interpretation. A.R. initiated and supervised the project and wrote the main manuscript along with the Supplementary Information with input from all co-authors.

References

[1] Pound, R.V.: Electronic frequency stabilization of microwave oscillators. Review of Scientific Instruments **17**(11), 490–505 (1946)

[2] Allan, D.W., *et al.*: Time and frequency(time-domain) characterization, estimation, and prediction of precision clocks and oscillators. IEEE transactions on ultrasonics, ferroelectrics, and frequency control **34**(6), 647–654 (1987)

[3] Ashby, N.: Relativity in the global positioning system. Living Reviews in relativity **6**(1), 1–42 (2003)

[4] Chou, C.-W., Hume, D.B., Rosenband, T., Wineland, D.J.: Optical clocks and relativity. Science **329**(5999), 1630–1633 (2010)

[5] Nagatsuma, T., Ducournau, G., Renaud, C.C.: Advances in terahertz communications accelerated by photonics. Nature Photonics **10**(6), 371–379 (2016)

[6] Valušis, G., Lisauskas, A., Yuan, H., Knap, W., Roskos, H.G.: Roadmap of terahertz imaging 2021. Sensors **21**(12), 4092 (2021)

[7] Djevahirdjian, L., Lechevallier, L., Martin-Drumel, M.-A., Pirali, O., Ducournau, G., Kassi, R., Kassi, S.: Frequency stable and low phase noise thz synthesis for precision spectroscopy. Nature Communications **14**(1), 7162 (2023)

[8] Greenberg, J., Heffernan, B.M., McGrew, W.F., Nose, K., Rolland, A.: Dual wavelength brillouin laser terahertz source stabilized to carbonyl sulfide rotational transition. Nature Communications **16**(1), 2411 (2025)

[9] Sasada, M., Collaboration, E.H.T., *et al.*: First m87 event horizon telescope results. i. the shadow of the supermassive black hole. The Astrophysical Journal Letters **875**(1), 1 (2019)

[10] Raymond, A.W., Doeleman, S.S., Asada, K., Blackburn, L., Bower, G.C., Bremer, M., Broguiere, D., Chen, M.-T., Crew, G.B., Dornbusch, S., *et al.*: First very long baseline interferometry detections at 870 μm. The Astronomical Journal **168**(3), 130 (2024)

[11] Fang, D., Drayss, D., Peng, H., Lihachev, G., Füllner, C., Kuzmin, A., Marin-Palomo, P., Matalla, P., Kharel, P., Wang, R.N., *et al.*: 320 ghz photonic-electronic analogue-to-digital converter (adc) exploiting kerr soliton microcombs. Light: Science & Applications **14**(1), 241 (2025)

[12] Schawlow, A.L., Townes, C.H.: Infrared and optical masers. Physical review **112**(6), 1940 (1958)

[13] Heffernan, B.M., Greenberg, J., Hori, T., Tanigawa, T., Rolland, A.: Brillouin laser-driven terahertz oscillator up to 3 thz with femtosecond-level timing jitter. Nature Photonics **18**(12), 1263–1268 (2024)

[14] Egbert, S.C., Greenberg, J., Heffernan, B.M., McGrew, W.F., Rolland, A.: Dual-wavelength brillouin lasers as compact opto-terahertz references for low-noise microwave synthesis. Optics Express **33**(20), 41777–41790 (2025)

[15] Suh, M.-G., Yang, Q.-F., Vahala, K.J.: Phonon-limited-linewidth of brillouin lasers at cryogenic temperatures. Physical review letters **119**(14), 143901 (2017)

[16] Ulanov, A.E., Ruhnke, B., Wildi, T., Herr, T.: Attosecond-level synchronisation of chip-integrated oscillators. arXiv preprint arXiv:2510.11630 (2025)

[17] Weng, W., Lucas, E., Lihachev, G., Lobanov, V.E., Guo, H., Gorodetsky, M.L., Kippenberg, T.J.: Spectral purification of microwave signals with disciplined dissipative kerr solitons. Physical review letters **122**(1), 013902 (2019)

[18] Wildi, T., Ulanov, A., Englebert, N., Voumard, T., Herr, T.: Sideband injection locking in microresonator frequency combs. APL photonics **8**(12) (2023)

[19] Moille, G., Stone, J., Chojnacky, M., Shrestha, R., Javid, U.A., Menyuk, C., Srinivasan, K.: Kerr-induced synchronization of a cavity soliton to an optical reference. Nature **624**(7991), 267–274 (2023)

[20] Sun, S., Harrington, M.W., Tabatabaei, F., Hanifi, S., Liu, K., Wang, J., Wang, B., Yang, Z., Liu, R., Morgan, J.S., et al.: Microcavity kerr optical frequency division with

integrated sin photonics. Nature Photonics, 1–6 (2025)

[21] Xie, X., Bouchand, R., Nicolodi, D., Giunta, M., Hänsel, W., Lezius, M., Joshi, A., Datta, S., Alexandre, C., Lours, M., *et al.*: Photonic microwave signals with zeptosecond-level absolute timing noise. nature photonics **11**(1), 44–47 (2017)

[22] Ishibashi, T., Ito, H.: Uni-traveling-carrier photodiodes. Journal of Applied Physics **127**(3) (2020)

[23] Rolland, A., Loas, G., Brunel, M., Frein, L., Vallet, M., Alouini, M.: Non-linear opto-electronic phase-locked loop for stabilization of opto-millimeter waves: towards a narrow linewidth tunable thz source. Optics express **19**(19), 17944–17950 (2011)

[24] Rubiola, E., Vernotte, F.: The Companion of the Enrico's Chart for Phase Noise and Two-Sample Variances. arXiv:2201.07109 [physics, physics:quant-ph] (2022). _eprint: 2201.07109

[25] Walls, F.L., Stein, S.R., Gray, J.E.: Design Considerations in State-of-the-Art Signal Processing and Phase Noise Measurement Systems. In: Proceedings of the 30th Annual Frequency Control Symposium, pp. 269–274 (1976)

[26] Zhang, S., Silver, J.M., Shang, X., Del Bino, L., Ridler, N.M., Del'Haye, P.: Terahertz wave generation using a soliton microcomb. Optics express **27**(24), 35257–35266 (2019)

[27] Tetsumoto, T., Ayano, F., Yeo, M., Webber, J., Nagatsuma, T., Rolland, A.: 300 ghz wave generation based on a kerr microresonator frequency comb stabilized to a low noise microwave reference. Optics Letters **45**(16), 4377–4380 (2020)

[28] Kwon, D., Jeong, D., Jeon, I., Lee, H., Kim, J.: Ultrastable microwave and soliton-pulse generation from fibre-photonic-stabilized microcombs. Nature Communications **13**(1), 381 (2022)

[29] Kudelin, I., Groman, W., Ji, Q.-X., Guo, J., Kelleher, M.L., Lee, D., Nakamura, T., McLemore, C.A., Shirmohammadi, P., Hanifi, S., *et al.*: Photonic chip-based low-noise microwave oscillator. Nature **627**(8004), 534–539 (2024)

[30] Jin, X., Xie, Z., Zhang, X., Hou, H., Wu, B., Zhang, F., Zhang, X., Chang, L., Gong, Q., Yang, Q.-F.: Microresonator-referenced soliton microcombs with zeptosecond-level timing noise. Nature Photonics, 1–7 (2025)

[31] Ji, Q.-X., Zhang, W., Savchenkov, A., Liu, P., Sun, S., Jin, W., Guo, J., Peters, J., Wu, L., Feshali, A., et al.: Dispersive-wave-agile optical frequency division. Nature Photonics, 1–6 (2025)

[32] Tetsumoto, T., Nagatsuma, T., Fermann, M.E., Navickaite, G., Geiselmann, M., Rolland, A.: Optically referenced 300 ghz millimetre-wave oscillator. Nature Photonics **15**(7), 516–522 (2021)

[33] Kuse, N., Nishimoto, K., Tokizane, Y., Okada, S., Navickaite, G., Geiselmann, M., Minoshima, K., Yasui, T.: Low phase noise thz generation from a fiber-referenced kerr microresonator soliton comb. Communications Physics **5**(1), 312 (2022)

[34] Briles, T.C., Yu, S.-P., Drake, T.E., Stone, J.R., Papp, S.B.: Generating Octave-Bandwidth Soliton Frequency Combs with Compact Low-Power Semiconductor Lasers. Physical Review Applied **14**(1), 014006 (2020) https://doi.org/10.1103/PhysRevApplied.14.014006

[35] Kuo, F.M., Shi, J.W., Chiang, H.C., Chuang, H.P., Chiou, H.K., Pan, C.L., Chen, N.W., Tsai, H.J., Huang, C.B.: Spectral power enhancement in a 100 GHz photonic millimeter-wave generator enabled by spectral line-by-line pulse shaping. IEEE Photonics Journal **2**(5), 719–727 (2010) https://doi.org/10.1109/JPHOT.2010.2064160

[36] Qian, C., Che, M., Kamiura, Y., Doi, R., Ishibashi, T., Mikami, Y., Kato, K.: 3-mw-output 300-ghz ultra-compact photonic thz-wave generator. In: 2024 IEEE Opto-Electronics and Communications Conference (OECC), pp. 1–3 (2024). https://doi.org/10.1109/OECC54135.2024.10975386

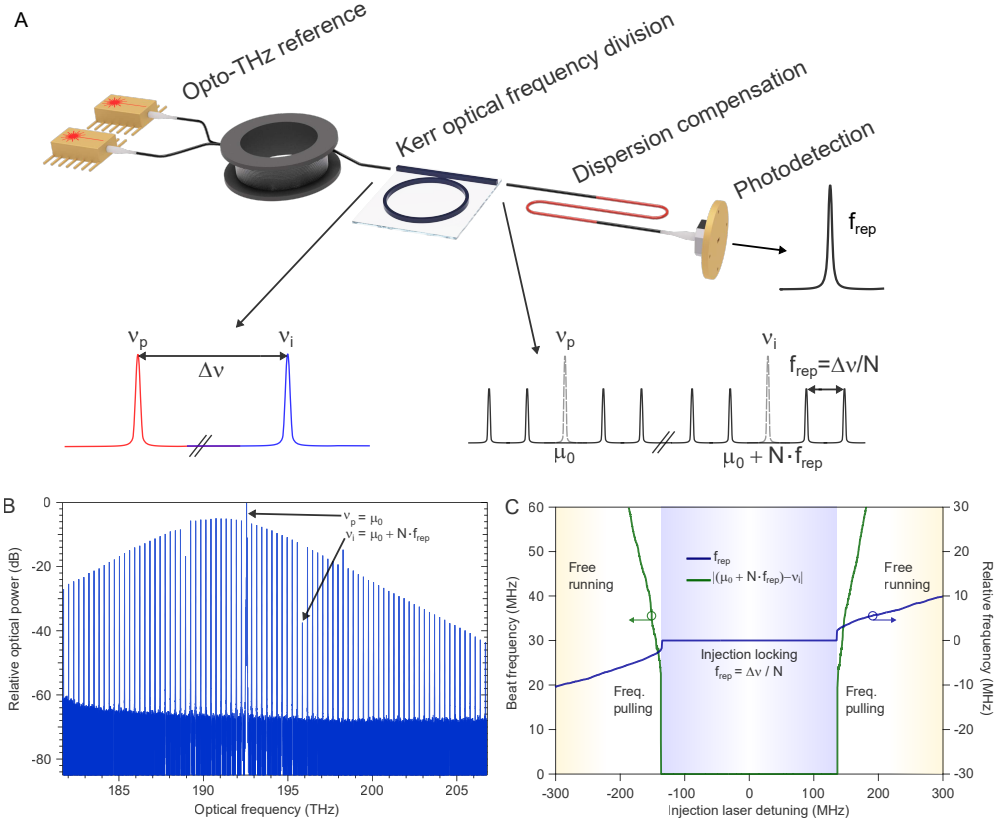


Fig. 1 Kerr optical frequency division of a multi-terahertz optical reference to 300 GHz. (A) Conceptual architecture of the oscillator. A dual-wavelength Brillouin laser (DWBL) provides two mutually coherent optical tones, ν_p and ν_i, separated by $\Delta\nu$ (opto-THz). These tones simultaneously pump and injection-lock a Kerr soliton microresonator, inducing optical frequency division such that the soliton repetition rate satisfies $f_{\mathrm{rep}} = \Delta\nu/N$. After spectral conditioning and dispersion compensation of the optical pulse train, photodetection converts the repetition rate directly into a millimeter-wave carrier. **(B) Optical spectrum of the Kerr soliton comb after suppression of the pump and injection tones.** The spectrum exhibits a smooth sech^2 envelope characteristic of dissipative Kerr solitons. The injected optical tone ν_i overlaps the comb line at $\mu_0 + N \cdot f_{\mathrm{rep}}$, dividing the optical reference. **(C) Injection-locking dynamics of Kerr optical frequency division.** As the detuning between the injected optical tone and the free-running comb mode is varied, the system transitions from free-running operation through frequency pulling into a robust injection-locked regime, where f_{rep} (blue) is pinned to $\Delta\nu/N$ and $\mu_0 + N \cdot f_{\mathrm{rep}} = \nu_i$ over a wide detuning range.

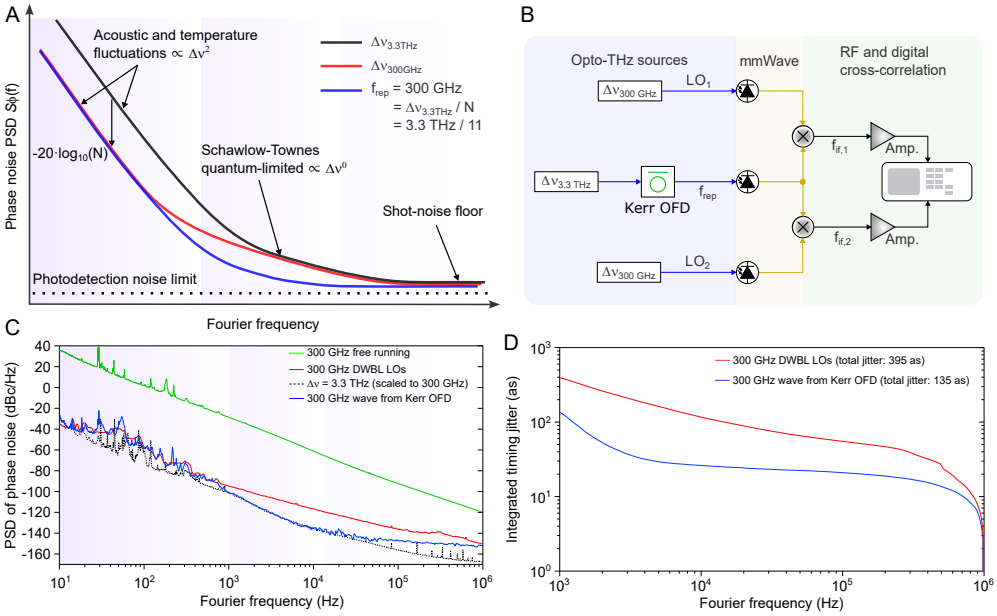


Fig. 2 Noise scaling and timing-jitter performance enabled by Kerr optical frequency division. (A) Conceptual phase-noise scaling for Kerr OFD of dual-wavelength Brillouin lasers. Optical separations $\Delta\nu_{3.3\,\mathrm{THz}}$ (black) and $\Delta\nu_{300\,\mathrm{GHz}}$ (red) highlight that low-frequency noise from acoustic and temperature fluctuations scales quadratically with optical separation, while the Schawlow–Townes contribution is independent of $\Delta\nu$. Dividing $\Delta\nu_{3.3\,\mathrm{THz}}$ down to $f_{\mathrm{rep}} = 300$ GHz suppresses the technical and quantum-limited phase noise by $20\log_{10}(N)$ until the photodetection noise floor is reached (blue). **(B) Cross-correlation phase-noise measurement architecture.** The 300 GHz millimeter-wave signal generated by Kerr optical frequency division (f_{rep}) is downconverted using two independent photonic local oscillators at 300 GHz (LO_1 and LO_2). Each LO is generated by optical heterodyne beating on a uni-traveling-carrier photodiode, converting the optical-frequency difference signals into millimeter-wave electrical local oscillators. The Kerr OFD signal is mixed with each LO to produce intermediate-frequency signals ($f_{\mathrm{if},1}$ and $f_{\mathrm{if},2}$) that are independently amplified and digitized. RF and digital cross-correlation between the two channels suppresses uncorrelated detection noise, enabling measurement of the phase noise of the Kerr OFD signal. **(C) Measured single-sideband phase-noise spectra at 300 GHz.** The Kerr OFD signal (blue) exhibits substantially lower phase noise than both a free-running soliton (green) and directly generated 300 GHz DWBL signals (red), closely following the scaled noise of $\Delta\nu_{3.3\,\mathrm{THz}}$. **(D) Integrated timing jitter derived from the measured phase-noise spectra.** Kerr OFD yields a total jitter of 135 as (1 kHz–1 MHz), compared to 395 as for directly generated 300 GHz DWBL signals.

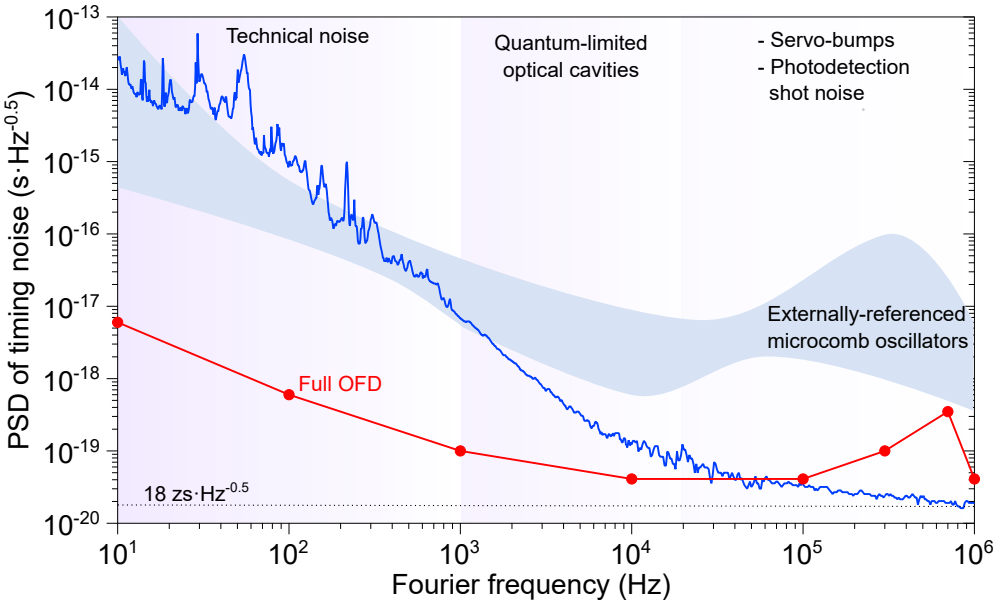


Fig. 3 Benchmarking timing-noise performance of a Kerr-induced optical frequency divider. Timing-noise power spectral density (PSD) of the Kerr OFD oscillator (blue) compared to other state-of-the-art oscillators. The Kerr OFD achieves timing noise of 18 zs/$\sqrt{\text{Hz}}$, with PSD values falling well below the technical noise of conventional 300 GHz dual-wavelength Brillouin lasers and approaching the quantum-limited regime. The results are benchmarked against full OFD [21] (red), which represents the quietest microwave signals demonstrated to date, and externally-referenced microcomb oscillators [28–33] (blue shaded band), which remain limited by servo bumps and photodetection shot noise. The Kerr OFD oscillator decisively surpasses all previous microcomb-based microwave and millimeter-wave demonstrations, achieving performance once reserved for full OFD but with radically reduced complexity.

Supplementary Files

This is a list of supplementary files associated with this preprint. Click to download.

- KOFDSM.pdf